Germline *De Novo* Mutations in *ATP1A1* Cause Renal Hypomagnesemia, Refractory Seizures, and Intellectual Disability

Karl P. Schlingmann,[1,16,*] Sascha Bandulik,[2,16] Cherry Mammen,[3,16] Maja Tarailo-Graovac,[4,16] Rikke Holm,[5] Matthias Baumann,[6] Jens König,[1] Jessica J.Y. Lee,[7] Britt Drögemöller,[7] Katrin Imminger,[2] Bodo B. Beck,[8,9,10] Janine Altmüller,[11] Holger Thiele,[11] Siegfried Waldegger,[6] William van't Hoff,[12] Robert Kleta,[12,13] Richard Warth,[2] Clara D.M. van Karnebeek,[14,15] Bente Vilsen,[5,16] Detlef Bockenhauer,[12,13,16] and Martin Konrad[1,16]

Over the last decades, a growing spectrum of monogenic disorders of human magnesium homeostasis has been clinically characterized, and genetic studies in affected individuals have identified important molecular components of cellular and epithelial magnesium transport. Here, we describe three infants who are from non-consanguineous families and who presented with a disease phenotype consisting of generalized seizures in infancy, severe hypomagnesemia, and renal magnesium wasting. Seizures persisted despite magnesium supplementation and were associated with significant intellectual disability. Whole-exome sequencing and conventional Sanger sequencing identified heterozygous *de novo* mutations in the catalytic Na^+, K^+-ATPase α1 subunit (*ATP1A1*). Functional characterization of mutant Na^+, K^+-ATPase α1 subunits in heterologous expression systems revealed not only a loss of Na^+, K^+-ATPase function but also abnormal cation permeabilities, which led to membrane depolarization and possibly aggravated the effect of the loss of physiological pump activity. These findings underline the indispensable role of the α1 isoform of the Na^+, K^+-ATPase for renal-tubular magnesium handling and cellular ion homeostasis, as well as maintenance of physiologic neuronal activity.

Magnesium is essential for numerous cellular processes, including energy metabolism, protein and nucleic acid synthesis, and the maintenance of the electrical potential of nervous tissues and cell membranes. Genetic investigations in children with inherited forms of hypomagnesemia could identify critical components of epithelial magnesium transport at the molecular level.[1] Affected children commonly present with seizures, muscle spasms, or tetany. In the majority of cases, magnesium supplementation leads to relief of clinical symptoms and allows for a normal motor and cognitive development despite persistence of subnormal serum magnesium levels. In contrast with this favorable clinical course, we noted a small group of nine children who, despite appropriate magnesium supplementation, experienced prolonged and repeated seizure activity associated with severe intellectual disability. Of this cohort, two individuals had previously been diagnosed with hypomagnesemia, seizures, and mental retardation [HOMGSMR, MIM: 616418] due to bi-allelic mutations in *CNNM2* [MIM: 607803].[2] Here, we identified heterozygous *de novo* mutations in *ATP1A1* [MIM: 182310] (RefSeqGene: NG_047036, GenBank: NM_000701), encoding the α1 isoform of Na^+, K^+-ATPase, in three children from this cohort. Data on clinical symptoms and biochemical measures at the time of disease manifestation were collected retrospectively from medical charts. Affected children with *ATP1A1* mutations were clinically reevaluated during follow-up, and biochemical data were obtained.

The three infants initially presented between 6 days and 6 months of age with generalized convulsions (Table 1, for the full dataset please refer to Table S1 in the Supplemental Data). At the time of manifestation, severe hypomagnesemia (0.30–0.36 mmol/L) was noted. Calculation of urinary fractional excretion rates of magnesium indicated massive renal magnesium wasting. Although urinary calcium excretion was not uniformly elevated, initial renal ultrasound examinations indicated medullary hyperechogenicity compatible with incipient nephrocalcinosis in individuals B-II-1 and C-II-2. All children were treated with antiepileptic drugs and received intravenous magnesium followed by ongoing oral supplementation. However, seizure activity persisted with frequent generalized seizures

[1]Department of General Pediatrics, University Children's Hospital, Münster 48149, Germany; [2]Medical Cell Biology, University of Regensburg, Regensburg 93053, Germany; [3]Division of Nephrology, Department of Pediatrics, University of British Columbia, Vancouver, BC V6H 3V4, Canada; [4]Departments of Biochemistry, Molecular Biology, and Medical Genetics, Cumming School of Medicine, Alberta Children's Hospital Research Institute, University of Calgary, Calgary, AB T2N 1N4, Canada; [5]Department of Biomedicine, Aarhus University, Aarhus 8000, Denmark; [6]Department of Pediatrics I, Medical University of Innsbruck, Innsbruck 6020, Austria; [7]Department of Medical Genetics, Centre for Molecular Medicine and Therapeutics, University of British Columbia, Vancouver, BC V6T 1Z3, Canada; [8]Institute of Human Genetics, University of Cologne, Cologne 50931, Germany; [9]Center for Molecular Medicine Cologne, Cologne 50931, Germany; [10]Center for Rare and hereditary Kidney Disease, Cologne 50931, Germany; [11]Cologne Center for Genomics, University of Cologne, Cologne 50931, Germany; [12]Department of Pediatric Nephrology, Great Ormond Street Hospital for Children NHS Foundation Trust, London WC1N 3JH, UK; [13]UCL Centre for Nephrology, London NW3 2PF, UK; [14]Department of Pediatrics, Centre for Molecular Medicine and Therapeutics, University of British Columbia, Vancouver, BC V6T 1Z3, Canada; [15]Departments of Pediatrics and Clinical Genetics, Amsterdam University Medical Center, Amsterdam, 1007, the Netherlands
[16]These authors contributed equally to this work.
*Correspondence: karlpeter.schlingmann@ukmuenster.de
https://doi.org/10.1016/j.ajhg.2018.10.004.

Table 1. Overview of Clinical Characteristics and Genotypes

	Individual		
	A-II-1	**B-II-1**	**C-II-2**
Demographics			
Origin	of European descent	of European descent	First Nations Canadian
Gender	female	female	male
Age at manifestation	6 months	2 months	6 days
First symptom	generalized seizures	generalized seizures	generalized seizures
Initial Laboratory Findings			
S-Mg (mmol/L) (0.75–1.1)	0.36	0.35	0.30
FE-Mg (%) (3-5%)	26.0	33.8	nd
Most Recent Findings			
Age at last follow-up	4 years	10 years	6 years
S-Mg (mmol/L) (0.75.-1.1)	0.57	0.28	0.62
FE-Mg (%) (3-5%)	15.3	27.0	21.3
seizure activity	repeated *status epilepticus*	monthly seizures	frequent seizures, repeated *status epilepticus*
neurological outcome	global developmental delay, hyperactive behavior	global developmental delay, suspected autism spectrum disorder	global developmental delay, speech delay, diagnosis of severe autism, self-biting behavior
***ATP1A1* Mutations**			
nucleotide level	c.905T>C	c.907G>C	c.2576T>G
protein level	p.Leu302Arg	p.Gly303Arg	p.Met859Arg

and repeated *status epilepticus* despite amelioration of serum magnesium levels. After a *status epilepticus* with both tonic-clonic seizure activity and hypoxemia for more than one hour, the cerebral magnetic resonance imaging (MRI) of individual A-II-1 showed bilateral parietooccipital cortical and subcortical diffusion restriction compatible with hypoxic ischemic encephalopathy. This resulted in a marked developmental setback and impaired vision. Follow-up MRI showed cerebral volume loss. All three children uniformly had significant global developmental delay, displayed limited motor skills, and spoke only in single words. Two individuals (B-II-1 and C-II-2) showed clinical features compatible with an autism spectrum disorder. MRI examinations revealed cerebral volume loss in individual C-II-2 also. Blood-pressure measurements repeatedly demonstrated normotension in all children, and cardiac examinations performed in individuals A-II-1 and C-II-2 were unremarkable. Individuals B-II-1 and C-II-2 exhibited significant polyuria of 4–8 ml/kg/h, but renal concentrating ability remained at least partially intact (random urine osmolalities of >400 mosmol/L). Although laboratory analyses did not reveal renal salt wasting or a significant activation of the renin-aldosterone system and serum potassium levels were mostly within the reference range, all affected individuals exhibited repeated episodes with significant hypokalemia ($S\text{-}K^+$ of 2.1 to 2.6 mmol/L). Calculation of the transtubular potassium gradient during hypokalemic episodes indicated renal potassium wasting. The most recent laboratory examinations in individuals A-II-1 and B-II-1 demonstrated persisting hypomagnesemia despite high doses of oral magnesium supplementation, and fractional urinary excretion rates of magnesium confirmed major renal magnesium wasting. Parents of all three children were clinically unaffected and showed normal serum magnesium levels.

Extraction of DNA from whole blood was performed according to standard protocols. All genetic studies were approved by the respective ethics committees of the involved centers. The parents provided written informed consent. The clinical phenotype initially suggested the diagnosis of hypomagnesemia with secondary hypocalcemia (HSH) [HOMG1, MIM: 602014]; however, mutations in *TRPM6* [MIM: 607009] were excluded.[3,4] Under the assumption of an unknown disease phenotype, we performed whole-exome sequencing in individual A-II-1 as well as the family C trio in order to identify the underlying genetic defect. Details on target enrichment, sequencing, and data analysis are provided in the Supplemental Data. We focused on missense, nonsense, splice-site, and frameshift variants upon all modes of inheritance. After performing sequential filtering and keeping variants predicted as pathogenic, we could identify no common gene with homozygous or compound-heterozygous variants in the two affected individuals. In contrast, both

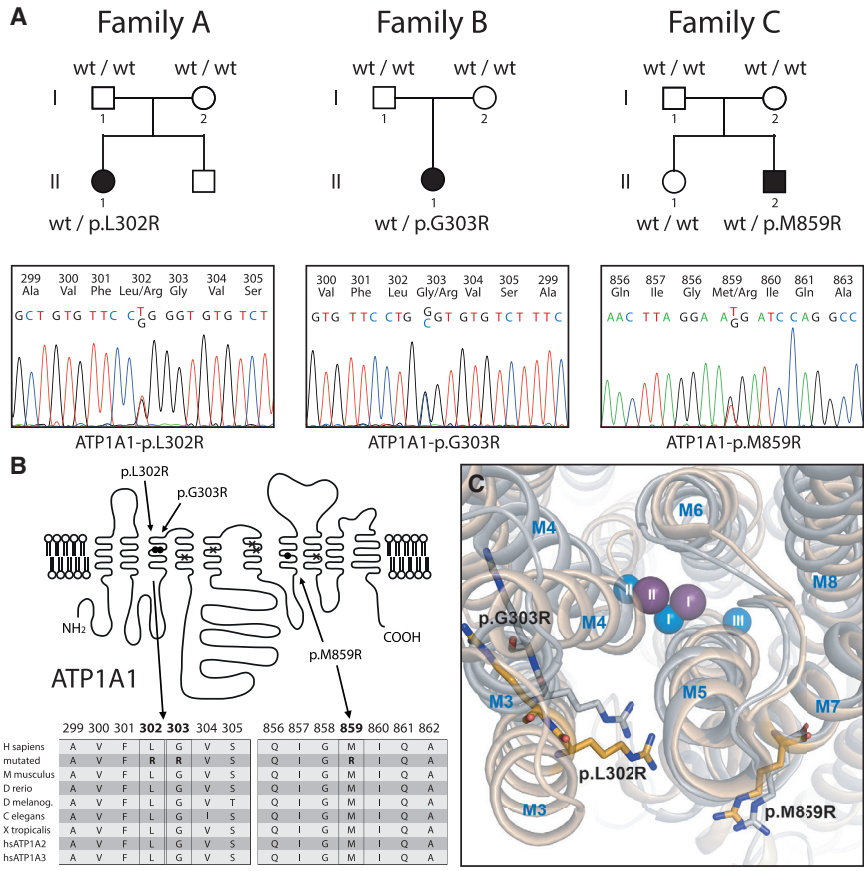

Figure 1. Family Pedigrees, Electropherograms of Identified *ATP1A1* Mutations, and Localization of Mutations Within the *ATP1A1* Protein (α1 Subunit of Na^+, K^+-ATPase) with Multiple Sequence Alignment

(A) Heterozygous *ATP1A1* mutations p.Leu302Arg (p.L302R), p.Gly303Arg (p.G303R), and p.Met859Arg (p.M859R) identified in the three individuals (A-II-1, B-II-1, and C-II-2) were not present in unaffected parents but occurred *de novo*.

(B) Whereas adjacent amino acid residues Leu302 and Gly303 are located within the third transmembrane domain, M859 lies within the seventh transmembrane helix of the encoded α1 subunit of Na^+, K^+-ATPase (filled circles). Crosses indicate ion-binding carboxylate residues (Glu334 in M4; Glu786 in M5; Asp811 and Asp815 in M6; and Asp933 in M8). A multiple-sequence alignment (RefSeq NP_000692, UniProt P05023) of *ATP1A1* amino acid residues surrounding mutated positions p.302, p.303, and p.859, respectively (bold), is shown. All three positions are highly conserved between species and between α subunit homologs *ATP1A1*, *ATP1A2*, and *ATP1A3*.

(C) Structural location of the arginine residues in mutants p.Leu302Arg, p.Gly303Arg, and p.Met859Arg. The arginines were inserted into the atomic models derived from crystal structures with Na^+ or K^+ bound. The central transmembrane domain of the α1 subunit, consisting of helices M3 to M8 with bound ions (Na^+ blue, K^+ purple, numbering according to conventional nomenclature) is shown as seen from the extracellular surface. The bulky arginines seem to be able to disturb the ion-binding sites I and II. The p.Gly303Arg arginine is predicted to collide with M4, whereas the p.Leu302Arg arginine most likely collides with M5, particularly in the K^+-bound form. Finally, the p.Met859Arg arginine might interact with an M7 glycine essential to the M7 kink that makes room for the binding of the K^+ ions.

were found to carry a single heterozygous mutation, c.905T>G (p.Leu302Arg) and c. 2576T>G (p.Met859Arg) in *ATP1A1*, respectively. *In silico* analyses predicted the variants to be pathogenic; they were predicted to affect highly conserved amino acid residues of the Na^+, K^+-ATPase α1 protein (Figure 1, Table S2). None of the identified mutations is listed in publicly available exome databases, i.e., ExAC and gnomAD browsers. Identified mutations were confirmed by Sanger sequencing (details of primers are available on request); the trio analysis of family C exomes as well as sequencing of the parents of individual A-II-1 demonstrated that both mutations occurred *de novo*. We could not identify any additional gene with heterozygous variants shared by both affected individuals (A-II-1 and C-II-2). Therefore, we do not have any genetic evidence that the phenotype observed here results from additive effects of variants in a gene other than *ATP1A1*. Subsequently, *ATP1A1* screening by conventional Sanger sequencing revealed that a third variant, c.907G>C (p.Gly303Arg), existed in a heterozygous state in individual B-II-1 but was not found in either parent and also occurred *de novo*. In families A and B, paternity was confirmed by analysis of seven independent polymorphic microsatellite markers. Paternity in family C was confirmed by segregation analysis of rare variants identified in the trio exome.

For biochemical studies, mutations were introduced into full-length cDNA encoding the ouabain-insensitive rat α1 isoform of Na^+, K^+-ATPase and expressed in COS-1 cells. Ouabain selection was used for obtaining stable viable cell lines.[5] However, although COS cells transfected with wild-type rat *Atp1a1* grew normally, several attempts to keep COS cells growing after transfection with mutant rat *Atp1a1* cDNA and under ouabain selection failed; this indicates that, in contrast to the wild-type enzyme, none of the three mutants (p.Leu302Arg, p.Gly303Arg, or p.Met859Arg) was able to carry out the Na^+ and K^+ transport required to support cell growth.

Therefore, transient expression was performed in the presence of siRNA to knock down endogenous Na^+, K^+-ATPase.[6] Leaky plasma membranes were assayed functionally by previously described methods[7] (details are provided in the Supplemental Data). Na^+, K^+-ATPase pump function follows the Post-Albers reaction cycle (Figure 2A), starting with phosphorylation after binding of intracellular Na^+, which facilitates "pumping" of Na^+ to the

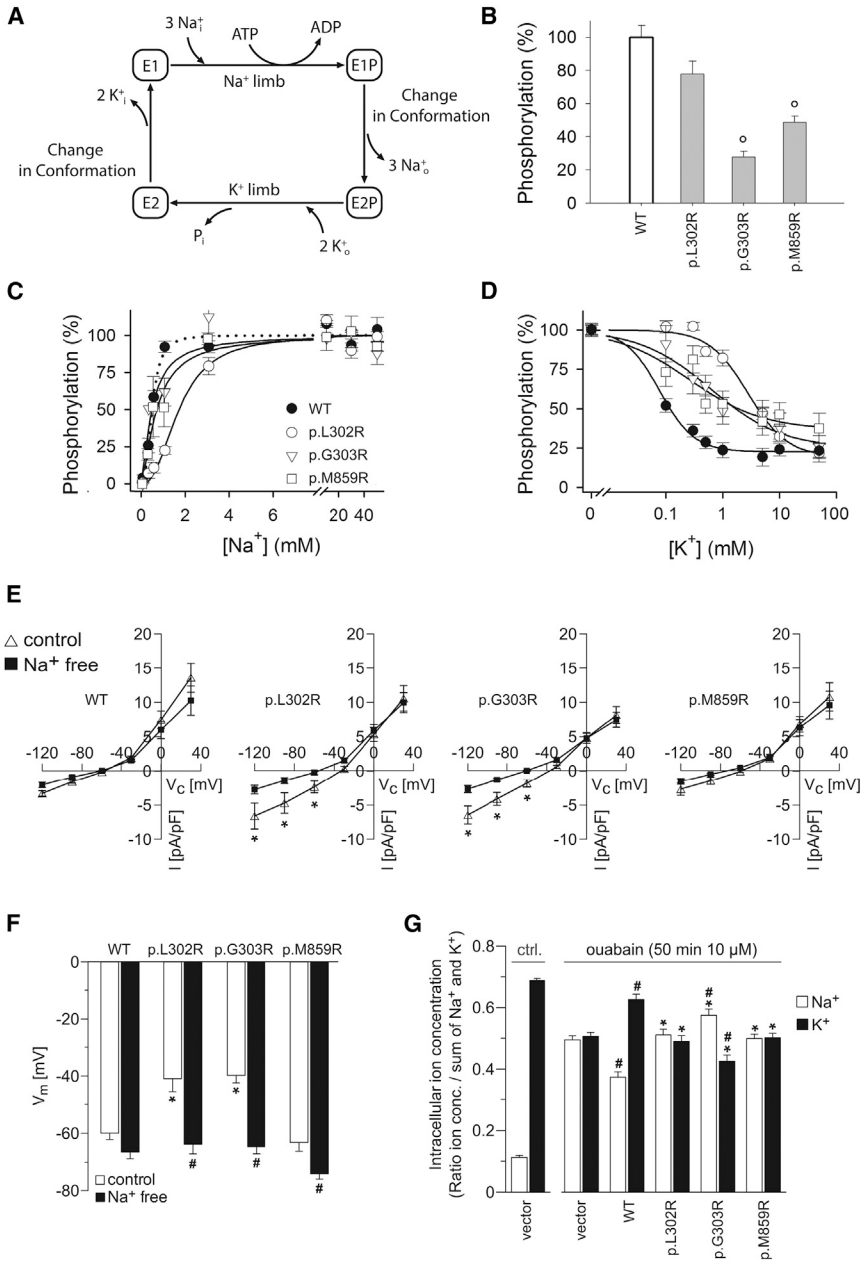

Figure 2. Functional Characterization of Mutant *ATP1A1* in Transfected Cells

Mutations corresponding to human *ATP1A1* p.Leu302Arg (p.L302R), p.Gly303Arg (p.G303R), and p.Met859Arg (p.M859R) were introduced in rat α1 Na^+, K^+-ATPase (rat *Atp1a1*), which is insensitive to the inhibitor ouabain.

(A) Post-Albers scheme of the Na^+, K^+-ATPase reaction cycle.

(B) Transient expression of mutant enzymes with concomitant siRNA-mediated knockdown of endogenous Na^+, K^+-ATPase. All three mutants were phosphorylated with [γ-^{32}P]-ATP in the Na^+ reaction, indicating expression of mutant proteins and the ability to perform the Na^+ limb of the Post-Albers reaction cycle (maximal phosphorylation signals relative to WT), albeit at a significantly reduced expression and/or phosphorylation level relative to that of WT, for p.Gly303Arg and p.Met859Arg ("o" = $p < 0.001$ for p.Gly303Arg and p.Met859Arg by a one-way ANOVA test; $p = 0.027$ for p.Leu302Arg; $n = 3–5$).

(C) Na^+ dependence of phosphorylation showing a significant 3.5-fold reduced affinity for Na^+ for p.Leu302Arg relative to WT, whereas the affinity was WT-like for p.Gly303Arg and p.Met859Arg, but with reduced cooperativity (see curves separated in different panels with statistics in Figure S1).

(D) K^+-sensitivity of the Na^+, K^+-ATPase phosphoenzyme intermediate. Symbols are the same as in (C). K^+ interaction was assessed by the ability of K^+ to inhibit phosphorylation. The Hill equation for inhibition was used for data fitting.[6] The cooperativity was WT-like for p.Leu302Arg (Hill coefficient 1.3–1.4), whereas the apparent affinity for K^+ of this mutant was reduced significantly ($p < 0.001$ by a one-way ANOVA test, $n = 8$), 36-fold relative to WT. For p.Gly303Arg and p.Met859Arg, the Hill coefficients were only 0.6–0.7, indicating loss of cooperativity between the two K^+ sites.

(E) Whole-cell currents of adrenal NCI-H295R cells expressing wild-type (WT) or different mutant (p.Leu302Arg, p.Gly303Arg, p.Met859Arg) ouabain-insensitive versions of rat *Atp1a1*. Compared to WT cells, mutant *Atp1a1*-expressing cells (except for mutant p.Met859Arg) displayed an abnormal current which was reduced after removal of Na^+, indicating an abnormal Na^+ permeability as causative for abnormal inward currents of Na^+ ions in mutant cells.

(F) Mutant-expressing NCI-H295R cells (except for mutant p.Met859Arg) had a depolarized membrane potential under control conditions but were hyperpolarized to the level of WT cells after removal of extracellular Na^+.

(G) Intracellular Na^+ and K^+ contents in cell lysates of HEK293 cells under control conditions and after treatment with the Na^+, K^+-ATPase inhibitor ouabain. Ouabain treatment strongly increased intracellular Na^+ and decreased intracellular K^+ in non-transfected cells. Expression of WT rat *Atp1a1* significantly attenuated these changes of intracellular Na^+ and K^+, whereas this was not the case for all mutant-expressing cells. Expression of the p.Gly303Arg mutant increased Na^+ and decreased K^+ even more in comparison to vector control cells. $n = 7–9$ per group.

(B–G) (all data are presented as means ± SEM).

outside, before binding of K^+, which, after dephosphorylation of the enzyme, is "pumped" into the cell. Measurements of phosphorylation under maximal conditions where the Na^+ sites were saturated and dephosphorylation was blocked with oligomycin demonstrated that all three mutants became phosphorylated, indicating that they were expressed, although at a significantly reduced level for p.Gly303Arg and p.Met859Arg, and that they were able to perform the Na^+ limb of the Post-Albers cycle (Figure 2B). A significantly reduced Na^+ affinity was, however, seen for the p.Leu302Arg mutant. The other two mutants showed reduced cooperativity of Na^+ binding, as

deduced from Hill coefficients (Figure 2C and Figure S1). The K^+ affinity was also significantly reduced for p.Leu302Arg, whereas the other two mutants showed less effect on K^+ affinity but reduced cooperativity of K^+ binding (Figure 2D). Determination of the E1P/E2P distribution by taking advantage of the ADP sensitivity of the phosphoenzyme showed no reduction of the level of E2P (Figure S2), indicating that the defective K^+ binding is a direct effect on K^+ interaction with the E2P state rather than a defect in the critical conformational change from E1P to E2P of Na^+, K^+-ATPase.

Next, electroporation was used for transfecting adrenocortical carcinoma NCI-H295R cells (Cell Line Service) as well as HEK293 cells with plasmids containing full-length cDNA sequences encoding wild-type or mutant ouabain-resistant rat *Atp1a1*. Transfected cells were identified with anti-CD8-coated dynabeads (Life Technologies). Whole-cell patch-clamp recordings were performed as described.[8] For the determination of intracellular Na^+ and K^+ contents, flame photometry was used.[8] Intracellular Na^+ and K^+ content was measured under control conditions and after treatment with 10 μM ouabain-inhibiting endogenous human Na^+, K^+-ATPase. Patch-clamp analyses of NCI-H295R cells expressing mutant *ATP1A1* constructs p.Leu302Arg and p.Gly303Arg revealed an abnormal Na^+ permeability compared to that of wild-type cells, as manifested by Na^+-dependent inward currents at negative voltages (Figure 2E). Moreover, cells expressing mutant *ATP1A1* p.Leu302Arg and p.Gly303Arg also showed a depolarized membrane potential in the presence of Na^+, but upon removal of extracellular Na^+, the membrane potential was hyperpolarized to the level of wild-type-expressing cells (Figure 2F). In these experiments, cells expressing the mutant p.Met859Arg were indistinguishable from wild-type-*ATP1A1*-expressing cells. Inhibition of endogenous Na^+, K^+-ATPase by ouabain produced pronounced changes in intracellular Na^+ and K^+ in HEK293 cells (Figure 2G). These changes were significantly attenuated after expression of wild-type rat *Atp1a1*, whereas all three mutants failed to compensate for the block of endogenous *ATP1A1*. Expression of mutant p.Gly303Arg led to even more pronounced disturbances of intracellular Na^+ and K^+ content compared to that in non-transfected cells, possibly reflecting abnormal ion fluxes (Figure 2G). Analyses of intracellular pH levels revealed an abnormal H^+ permeability and significant changes of intracellular pH upon alteration of extracellular pH for mutant p.Leu302Arg (Figure S3).

The Na^+, K^+-ATPase is an integral membrane protein that catalyzes the transport of three Na^+ ions out of and two K^+ ions into the cell at the expense of one molecule of ATP. It generates the electrochemical driving force that powers essential functions, such as neuronal firing, muscle contraction, and transepithelial ion transport. The Na^+, K^+-ATPase is a heterodimer consisting of α and β subunits and is complemented by auxiliary FXYD proteins.[9] The catalytic α subunit binds translocating Na^+ and K^+ as well as ATP, coupling ionic movements across the cell membrane to ATP hydrolysis.[10] In mammals, there exist four α isoforms that are expressed in a developmental- and tissue-specific manner, suggesting specific functional roles (α1–α4, *ATP1A1–ATP1A4*).[11,12] The ubiquitously expressed α1 subunit (*ATP1A1*) represents the major α isoform in the kidney and is present in virtually all cell types and structures of the central nervous system (CNS).[11]

Others studied the effects of a targeted disruption of α1 (*ATP1A1*) almost 20 years ago in mice; the focus then was on the cardiac phenotype.[13] Bi-allelic knock-out of *ATP1A1* led to early fetal lethality, suggesting that complete loss of *ATP1A1* function is not compatible with life. In contrast, heterozygous mice were fertile and generally healthy; however, they exhibited a hypocontractile cardiac phenotype mimicking cardiac glycoside toxicity.[13] The severe phenotype in the affected children differs from these heterozygous ($Atp1a1^{+/-}$) mice. The cardiac examination of the affected children did not reveal any pathologic findings, possibly indicating inter-species differences or suggesting compensatory mechanisms in the human heart. Seizures and hypomagnesemia have not been reported in ($Atp1a1^{+/-}$) mice; however, they represent pivotal findings in the affected children.

Hypomagnesemia in the affected individuals presented here is caused by massive renal Mg^{2+} wasting. Within the nephron, the distal convoluted tubule (DCT) represents the segment mediating active transcellular Mg^{2+} transport. Here, the basolaterally expressed Na^+, K^+-ATPase establishes favorable electrochemical gradients for apical cation influx through Mg^{2+}-permeable ion channels and also provides the exit mechanism for reabsorbed Na^+ ions. The DCT exhibits the highest density and activity of the Na^+, K^+-ATPase; α1 (*ATP1A1*) represents the predominating α isoform.[14] The critical role of Na^+, K^+-ATPase activity for Mg^{2+} reabsorption in the DCT has already been highlighted by the discovery of genetic defects in its auxiliary γ subunit (encoded by *FXYD2* [MIM: 601814]) in persons with dominant hypomagnesemia [HOMG2, MIM: 154020],[15] as well as by the hypomagnesemia observed in individuals with SeSAME (EAST) syndrome [SESAMES, MIM: 612780].[16] This autosomal-recessive disorder is caused by mutations in *KCNJ10* [MIM: 602208], encoding the Kir4.1 potassium channel that is co-expressed basolaterally in the DCT and recycles K^+ as a prerequisite for maintenance of Na^+, K^+-ATPase activity.

Despite considerable variability, serum Mg^{2+} levels in the affected children remained persistently low during follow-up despite a high dose oral Mg^{2+} supplementation (Table 1). Individuals with genetic defects in *TRPM6* or *FXYD2* also present with seizures; however, in these individuals, Mg^{2+} supplementation usually leads to a rapid cessation of epileptic activity, and physical and mental development are generally undisturbed even though Mg^{2+} levels remain subnormal.[17] In contrast, the children with *ATP1A1* defects exhibited persistent seizures and

uniformly developed significant intellectual disability. Therefore, the neurologic phenotype has to be considered as a primary feature of *ATP1A1* deficiency due to a genuine disturbance of Na^+, K^+-ATPase function in the CNS. Here, α1 is ubiquitously expressed and thought to maintain neuronal housekeeping functions, whereas the α3 isoform potentially acts as a reserve pump that is only required during phases of increased intracellular Na^+ concentrations, i.e., after repeated action potentials.[11,18] Expression of the α2 isoform is restricted to astrocytes and developing neurons. In the CNS, constant Na^+, K^+-ATPase activity is required for generating the resting membrane potential and for buffering and clearance of extracellular K^+ transients during neuronal activity.[19] Decreases in Na^+, K^+-ATPase activity have been detected in animal models of epilepsy and in forms of human myoclonus epilepsy and mitochondrial disorders.[20–22] Moreover, pharmacologic inhibition of neuronal Na^+, K^+-ATPase by cardiac glycosides provokes seizures in rats,[23] and changes in membrane potential and epileptic bursting activity were detected after the blocking of Na^+, K^+-ATPase activity by ouabain *in vitro*.[24]

Very recently, germline mutations in *ATP1A1* have been reported in individuals with Charcot-Marie-Tooth type 2 disease (CMT2) [CMT2DD, MIM: 618036].[25] Combining extensive data from different exome sequencing projects, the authors identified heterozygous *ATP1A1* missense mutations in seven CMT2-affected families. Segregation analyses were compatible with dominant inheritance. In accordance with the peripheral nervous system (PNS) phenotype, strong α1 expression was demonstrated in axolemma and myelin sheaths of sensory and motor neurons. The identified missense mutations affect conserved amino acid residues in different regions of the α1 protein. Interestingly, a mutational clustering is observed within the helical linker region (residues 592–608). Mutations in this region have been shown to reduce the rate of E1P to E2P conformational transition during the Post-Albers reaction cycle, but without completely blocking the conversion.[26] Ouabain survival assays demonstrated a significant decrease in cell viability, and functional studies in *Xenopus* oocytes showed a significant Na^+-current reduction compatible with a deleterious effect on Na^+, K^+-ATPase ion-transport function.[25]

In contrast to findings in these previously reported CMT2-affected families, the clinical evaluation of the affected children with *de novo ATP1A1* mutations did not reveal any signs of peripheral neuropathy. This phenotypic discrepancy could possibly be attributed to the relatively young age of the children; the age of onset of clinical symptoms in the previously reported CMT2-affected families varied between 8 and 50 years of age.[25] Conversely, data on serum magnesium levels as well as a potential concomitant epileptic phenotype were not reported in the CMT2-affected families. Yet, the authors detail migraine headaches in one CMT2-affected family and explicitly note the possibility of combined CNS and PNS symptoms and an expanding spectrum of phenotypes associated with *ATP1A1* mutations. Clearly, the predominant renal and CNS symptoms as well as the unfavorable clinical course of the children presented here with profound intellectual disability indicate a distinct clinical entity caused by *ATP1A1* defects.

Such a pleiotropic effect with variable phenotypes has already been described for mutations in the Na^+, K^+-ATPase homologs α2 and α3 (*ATP1A2* [MIM: 182340] and *ATP1A3* [MIM: 182350]). The disease spectrum caused by germline mutations in these two isoforms comprises familial forms of migraine (MHP2, MIM: 602481), alternating hemiplegia of childhood (AHC1 [MIM: 104290] and AHC2, [614820]), and rapid-onset dystonia parkinsonism (DYT12, MIM: 128235), as well as CAPOS syndrome [CAPOS, MIM: 601338], a complex neurological disorder comprising cerebellar ataxia, optic atrophy, and sensorineural hearing loss.[27–30] Interestingly, similar or even identical *ATP1A3* mutations are associated with variable phenotypes, indicating that genetic, epigenetic, or environmental modifiers might play a role. Functional analyses of mutated *ATP1A2* co-expressed with wild-type constructs suggested a functional haploinsufficiency rather than a dominant-negative effect.[27] Established mouse models for both genes recapitulate critical features of the human phenotype.[21,31] Interestingly, a knock-in mouse model with the engineered ATP1A2 variant p.Gly301Arg, which is orthologous to the ATP1A1 p.Gly303Arg variant identified in individual B-II-1, was produced recently, and heterozygous mice recapitulated the severe human MHP2 phenotype associated with this mutation.[32] Together, the *in vitro* and animal data argue for a complete loss of function of the mutated allele.[32–34]

Seizures, cognitive deficits, developmental delay, and psychiatric manifestations are known co-morbidities of the mentioned disorders.[29,35] Therefore, impaired Na^+, K^+-ATPase function in the CNS might cause epileptic seizures regardless of the specific α isoform affected. In line with this assumption, even small reductions in Na^+, K^+-ATPase pump activity were shown to be able to trigger epileptic seizures.[36]

The *ATP1A1* mutations identified here affect amino acid residues in the vicinity of the Na^+ and K^+ ion-binding residues of the Na^+, K^+-ATPase enzyme (Figures 1B and 1C). In line with the structural analyses, our functional studies indicate a disturbed Na^+ and K^+ binding, resulting in a loss of ATPase function; namely, Na^+ and K^+ transport activities were severely impaired in all three mutants Furthermore, a reduced expression level (particularly for p.Gly303Arg, *cf.* Figure 2B) could play a role in pathogenesis. Notably, p.Leu302Arg showed a strong effect on the affinity for both Na^+ and K^+, whereas p.Gly303Arg and p.Met859Arg mutants disrupted cooperativity between the sites for both Na^+ and K^+, suggesting a defective function of the so-called sites I and II that interact sequentially with Na^+ and K^+ during the pump cycle. Moreover, leak currents, and abnormal H^+ permeabilities were observed

for mutant p.Gly303Arg upon overexpression of p.Leu302Arg. These abnormal ion fluxes that transform the Na^+, K^+-ATPase into a passive ion channel might add to the pathogenesis of the severe phenotype reported here and could explain the phenotypic differences between the affected children and (*Atp1a1*$^{+/-}$) mice, which lack one copy of *Atp1a1*, as well as CMT2-affected individuals who harbor *ATP1A1* missense mutations impairing the E1P to E2P conformational transition during the Post-Albers reaction cycle.

Interestingly, a similar neomorphic effect with inward leak currents carried by H^+ and Na^+ has also been postulated for somatic *ATP1A1* mutations identified in aldosterone-producing adenomas (APAs) in individuals with arterial hypertension.[6,37] Because of these genetic and functional similarities, we also specifically evaluated the affected children for the presence of primary aldosteronism. Though we observed episodes of hypokalemia and elevated serum bicarbonate concentrations, typical APA findings such as suppressed renin levels or increased blood pressure were lacking in the young children presented here.

In conclusion, we describe a clinical entity comprising hypomagnesemia, refractory seizures, and severe intellectual disability associated with heterozygous *de novo* mutations in *ATP1A1,* encoding the α1 subunit of Na^+, K^+-ATPase. *ATP1A1* defects should be suspected in hypomagnesemic individuals presenting with seizures and developmental delay, especially if the epilepsy does not respond to an amelioration of hypomagnesemia. Our observations demonstrate further genetic heterogeneity among renal magnesium wasting disorders and underline the crucial role of basolateral Na^+, K^+-ATPase for tubular magnesium reabsorption. Furthermore, these findings illustrate the critical role of the α1 subunit of Na^+, K^+-ATPase for the maintenance of ionic gradients, the generation of resting membrane potential, and the termination of neuronal activity in the central nervous system; they also illustrate the pleiotropic effects associated with this subunit's dysfunction. Understanding the molecular basis provides a platform for further studies on the pathogenesis and potential treatment of hypomagnesemia, epilepsy, and intellectual disability.

Supplemental Data

Supplemental Data include three figures, supplemental Methods and Results, and two tables and can be found with this article online at https://doi.org/10.1016/j.ajhg.2018.10.004.

Acknowledgments

We are grateful to the children and their families for their participation in this study. We would like to acknowledge the following clinicians and laboratory scientists involved in the management of the children and molecular studies: Xiaohua Han, Ruth Giesbrecht, Dora Pak, Michelle Higginson, Aisha Ghani, Colin J. Ross, and Wyeth W. Wasserman. Individual C-II-2 was part of the Treatable Intellectual Disability Endeavour (TIDE) with funding support from the B.C Children's Hospital Foundation as "1st Collaborative Area of Innovation" (www.tidebc.org); Genome British Columbia (grant number SOF-195); the Canadian Institutes of Health Research (grant number 301221); and informatics infrastructure supported by Genome British Columbia and Genome Canada (ABC4DE Project). C.D.M.v.K. is a recipient of the Michael Smith Foundation for Health Foundation Research Scholar Award. The work was supported by grants to B.V. from the Lundbeck Foundation (grant number R223-2016-595) and the Danish Medical Research Council (grant number 7016-00193B). Support to D.B. and R.K. was provided by Kids Kidney Research; Kidney Research UK; St Peter's Trust for Kidney Bladder and Prostate Research; The David and Elaine Potter Foundation; and the European Union, 7th Framework Program (grant agreement 2012-305608 "European Consortium for High-Throughput Research in Rare Kidney Diseases (EURenOmics)." S.B. and R.W. were supported by the "Deutsche Forschungsgemeinschaft" (BA4436/2-1 to S.B. and SFB699 to R.W.). K.P.S. and M.K. received support from the Hans-Joachim-Bodlee Foundation.

Declaration of Interests

The authors declare no competing interests.

Received: June 13, 2018
Accepted: October 1, 2018
Published: November 1, 2018

Web Resources

CADD (Combined Annotation Dependent Depletion), https://cadd.gs.washington.edu/
ExAC (Exome Aggregation Consortium), http://exac.broadinstitute.org
GnomAD (Genome Aggregation Database), http://gnomad.broadinstitute.org
OMIM (Online Mendelian Inheritance in Man), http://www.omim.org
PolyPhen2, http://genetics.bwh.harvard.edu/pph2
SIFT (Sorting Intolerant From Tolerant), http://sift.bii.a-star.edu.sg

References

1. Viering, D.H.H.M., de Baaij, J.H.F., Walsh, S.B., Kleta, R., and Bockenhauer, D. (2017). Genetic causes of hypomagnesemia, a clinical overview. Pediatr. Nephrol. *32*, 1123–1135.
2. Arjona, F.J., de Baaij, J.H., Schlingmann, K.P., Lameris, A.L., van Wijk, E., Flik, G., Regele, S., Korenke, G.C., Neophytou, B., Rust, S., et al. (2014). CNNM2 mutations cause impaired brain development and seizures in patients with hypomagnesemia. PLoS Genet. *10*, e1004267.
3. Schlingmann, K.P., Weber, S., Peters, M., Niemann Nejsum, L., Vitzthum, H., Klingel, K., Kratz, M., Haddad, E., Ristoff, E., Dinour, D., et al. (2002). Hypomagnesemia with secondary hypocalcemia is caused by mutations in TRPM6, a new member of the TRPM gene family. Nat. Genet. *31*, 166–170.
4. Walder, R.Y., Landau, D., Meyer, P., Shalev, H., Tsolia, M., Borochowitz, Z., Boettger, M.B., Beck, G.E., Englehardt, R.K., Carmi, R., and Sheffield, V.C. (2002). Mutation of TRPM6

causes familial hypomagnesemia with secondary hypocalcemia. Nat. Genet. *31*, 171–174.
5. Vilsen, B. (1993). Glutamate 329 located in the fourth transmembrane segment of the alpha-subunit of the rat kidney Na+,K+-ATPase is not an essential residue for active transport of sodium and potassium ions. Biochemistry *32*, 13340–13349.
6. Beuschlein, F., Boulkroun, S., Osswald, A., Wieland, T., Nielsen, H.N., Lichtenauer, U.D., Penton, D., Schack, V.R., Amar, L., Fischer, E., et al. (2013). Somatic mutations in ATP1A1 and ATP2B3 lead to aldosterone-producing adenomas and secondary hypertension. Nat. Genet. *45*, 440–444, e1–e2.
7. Toustrup-Jensen, M., Hauge, M., and Vilsen, B. (2001). Mutational effects on conformational changes of the dephospho- and phospho-forms of the Na+,K+-ATPase. Biochemistry *40*, 5521–5532.
8. Tauber, P., Aichinger, B., Christ, C., Stindl, J., Rhayem, Y., Beuschlein, F., Warth, R., and Bandulik, S. (2016). Cellular pathophysiology of an adrenal adenoma-associated mutant of the plasma membrane Ca(2+)-ATPase ATP2B3. Endocrinology *157*, 2489–2499.
9. Sweadner, K.J., Arystarkhova, E., Donnet, C., and Wetzel, R.K. (2003). FXYD proteins as regulators of the Na,K-ATPase in the kidney. Ann. N Y Acad. Sci. *986*, 382–387.
10. Post, R.L., Hegyvary, C., and Kume, S. (1972). Activation by adenosine triphosphate in the phosphorylation kinetics of sodium and potassium ion transport adenosine triphosphatase. J. Biol. Chem. *247*, 6530–6540.
11. Blanco, G. (2005). Na,K-ATPase subunit heterogeneity as a mechanism for tissue-specific ion regulation. Semin. Nephrol. *25*, 292–303.
12. Lingrel, J.B. (1992). Na,K-ATPase: isoform structure, function, and expression. J. Bioenerg. Biomembr. *24*, 263–270.
13. James, P.F., Grupp, I.L., Grupp, G., Woo, A.L., Askew, G.R., Croyle, M.L., Walsh, R.A., and Lingrel, J.B. (1999). Identification of a specific role for the Na,K-ATPase alpha 2 isoform as a regulator of calcium in the heart. Mol. Cell *3*, 555–563.
14. Lücking, K., Nielsen, J.M., Pedersen, P.A., and Jørgensen, P.L. (1996). Na-K-ATPase isoform (alpha 3, alpha 2, alpha 1) abundance in rat kidney estimated by competitive RT-PCR and ouabain binding. Am. J. Physiol. *271*, F253–F260.
15. Meij, I.C., Koenderink, J.B., van Bokhoven, H., Assink, K.F., Groenestege, W.T., de Pont, J.J., Bindels, R.J., Monnens, L.A., van den Heuvel, L.P., and Knoers, N.V. (2000). Dominant isolated renal magnesium loss is caused by misrouting of the Na(+),K(+)-ATPase gamma-subunit. Nat. Genet. *26*, 265–266.
16. Bockenhauer, D., Feather, S., Stanescu, H.C., Bandulik, S., Zdebik, A.A., Reichold, M., Tobin, J., Lieberer, E., Sterner, C., Landoure, G., et al. (2009). Epilepsy, ataxia, sensorineural deafness, tubulopathy, and KCNJ10 mutations. N. Engl. J. Med. *360*, 1960–1970.
17. Schlingmann, K.P., Sassen, M.C., Weber, S., Pechmann, U., Kusch, K., Pelken, L., Lotan, D., Syrrou, M., Prebble, J.J., Cole, D.E., et al. (2005). Novel TRPM6 mutations in 21 families with primary hypomagnesemia and secondary hypocalcemia. J. Am. Soc. Nephrol. *16*, 3061–3069.
18. Munzer, J.S., Daly, S.E., Jewell-Motz, E.A., Lingrel, J.B., and Blostein, R. (1994). Tissue- and isoform-specific kinetic behavior of the Na,K-ATPase. J. Biol. Chem. *269*, 16668–16676.
19. Larsen, B.R., Stoica, A., and MacAulay, N. (2016). Managing brain extracellular K(+) during neuronal activity: the physiological role of the Na(+)/K(+)-ATPase subunit isoforms. Front. Physiol. *7*, 141.
20. Marquezan, B.P., Funck, V.R., Oliveira, C.V., Pereira, L.M., Araújo, S.M., Zarzecki, M.S., Royes, L.F., Furian, A.F., and Oliveira, M.S. (2013). Pentylenetetrazol-induced seizures are associated with Na^+,K^+-ATPase activity decrease and alpha subunit phosphorylation state in the mice cerebral cortex. Epilepsy Res. *105*, 396–400.
21. Clapcote, S.J., Duffy, S., Xie, G., Kirshenbaum, G., Bechard, A.R., Rodacker Schack, V., Petersen, J., Sinai, L., Saab, B.J., Lerch, J.P., et al. (2009). Mutation I810N in the alpha3 isoform of Na+,K+-ATPase causes impairments in the sodium pump and hyperexcitability in the CNS. Proc. Natl. Acad. Sci. USA *106*, 14085–14090.
22. Bindoff, L.A., and Engelsen, B.A. (2012). Mitochondrial diseases and epilepsy. Epilepsia *53* (*Suppl 4*), 92–97.
23. Donaldson, J., St Pierre, T., Minnich, J., and Barbeau, A. (1971). Seizures in rats associated with divalent cation inhibition of NA + -K + -ATP'ase. Can. J. Biochem. *49*, 1217–1224.
24. Vaillend, C., Mason, S.E., Cuttle, M.F., and Alger, B.E. (2002). Mechanisms of neuronal hyperexcitability caused by partial inhibition of Na+-K+-ATPases in the rat CA1 hippocampal region. J. Neurophysiol. *88*, 2963–2978.
25. Lassuthova, P., Rebelo, A.P., Ravenscroft, G., Lamont, P.J., Davis, M.R., Manganelli, F., Feely, S.M., Bacon, C., Brožková, D.S., Haberlova, J., et al. (2018). Mutations in ATP1A1 Cause Dominant Charcot-Marie-Tooth Type 2. Am. J. Hum. Genet. *102*, 505–514.
26. Clarke, D.M., Loo, T.W., and MacLennan, D.H. (1990). Functional consequences of alterations to amino acids located in the nucleotide binding domain of the Ca2(+)-ATPase of sarcoplasmic reticulum. J Biol Chem. *265*, 22223–22227.
27. De Fusco, M., Marconi, R., Silvestri, L., Atorino, L., Rampoldi, L., Morgante, L., Ballabio, A., Aridon, P., and Casari, G. (2003). Haploinsufficiency of ATP1A2 encoding the Na+/K+ pump alpha2 subunit associated with familial hemiplegic migraine type 2. Nat. Genet. *33*, 192–196.
28. de Carvalho Aguiar, P., Sweadner, K.J., Penniston, J.T., Zaremba, J., Liu, L., Caton, M., Linazasoro, G., Borg, M., Tijssen, M.A., Bressman, S.B., et al. (2004). Mutations in the Na+/K+ -ATPase alpha3 gene ATP1A3 are associated with rapid-onset dystonia parkinsonism. Neuron *43*, 169–175.
29. Heinzen, E.L., Arzimanoglou, A., Brashear, A., Clapcote, S.J., Gurrieri, F., Goldstein, D.B., Jóhannesson, S.H., Mikati, M.A., Neville, B., Nicole, S., et al.; ATP1A3 Working Group (2014). Distinct neurological disorders with ATP1A3 mutations. Lancet Neurol. *13*, 503–514.
30. Demos, M.K., van Karnebeek, C.D., Ross, C.J., Adam, S., Shen, Y., Zhan, S.H., Shyr, C., Horvath, G., Suri, M., Fryer, A., et al.; FORGE Canada Consortium (2014). A novel recurrent mutation in ATP1A3 causes CAPOS syndrome. Orphanet J. Rare Dis. *9*, 15.
31. Gritz, S.M., and Radcliffe, R.A. (2013). Genetic effects of ATP1A2 in familial hemiplegic migraine type II and animal models. Hum. Genomics *7*, 8.
32. Bøttger, P., Glerup, S., Gesslein, B., Illarionova, N.B., Isaksen, T.J., Heuck, A., Clausen, B.H., Füchtbauer, E.M., Gramsbergen, J.B., Gunnarson, E., et al. (2016). Glutamate-system defects behind psychiatric manifestations in a familial hemiplegic migraine type 2 disease-mutation mouse model. Sci. Rep. *6*, 22047.

33. Spadaro, M., Ursu, S., Lehmann-Horn, F., Veneziano, L., Antonini, G., Giunti, P., Frontali, M., and Jurkat-Rott, K. (2004). A G301R Na+/K+ -ATPase mutation causes familial hemiplegic migraine type 2 with cerebellar signs. Neurogenetics *5*, 177–185.
34. Santoro, L., Manganelli, F., Fortunato, M.R., Soldovieri, M.V., Ambrosino, P., Iodice, R., Pisciotta, C., Tessa, A., Santorelli, F., and Taglialatela, M. (2011). A new Italian FHM2 family: clinical aspects and functional analysis of the disease-associated mutation. Cephalalgia *31*, 808–819.
35. Deprez, L., Weckhuysen, S., Peeters, K., Deconinck, T., Claeys, K.G., Claes, L.R., Suls, A., Van Dyck, T., Palmini, A., Matthijs, G., et al. (2008). Epilepsy as part of the phenotype associated with ATP1A2 mutations. Epilepsia *49*, 500–508.
36. Krishnan, G.P., Filatov, G., Shilnikov, A., and Bazhenov, M. (2015). Electrogenic properties of the Na^+/K^+ ATPase control transitions between normal and pathological brain states. J. Neurophysiol. *113*, 3356–3374.
37. Azizan, E.A., Poulsen, H., Tuluc, P., Zhou, J., Clausen, M.V., Lieb, A., Maniero, C., Garg, S., Bochukova, E.G., Zhao, W., et al. (2013). Somatic mutations in ATP1A1 and CACNA1D underlie a common subtype of adrenal hypertension. Nat. Genet. *45*, 1055–1060.

The American Journal of Human Genetics, Volume *103*

Supplemental Data

Germline *De Novo* Mutations in *ATP1A1* Cause Renal Hypomagnesemia, Refractory Seizures, and Intellectual Disability

Karl P. Schlingmann, Sascha Bandulik, Cherry Mammen, Maja Tarailo-Graovac, Rikke Holm, Matthias Baumann, Jens König, Jessica J.Y. Lee, Britt Drögemöller, Katrin Imminger, Bodo B. Beck, Janine Altmüller, Holger Thiele, Siegfried Waldegger, William van't Hoff, Robert Kleta, Richard Warth, Clara D.M. van Karnebeek, Bente Vilsen, Detlef Bockenhauer, and Martin Konrad

SUPPLEMENTAL DATA

FIGURE S1:

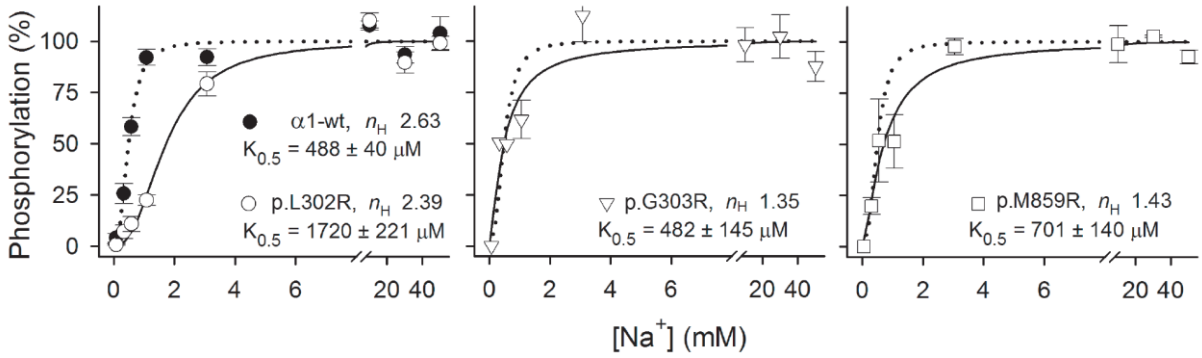

Figure S1: The Na^+ dependence of phosphorylation from figure 2C shown in separate panels for the three mutants with statistics. Error bars indicate SEM for the independent experimental points (n = 4-5). The indicated Hill coefficients (n_H) and $K_{0.5}$ values with SEM values were obtained by fitting the Hill equation [1] to the data, resulting in the lines shown. The 3.5-fold loss of affinity (reduced $K_{0.5}$) for p.Leu302Arg (p.L302R) is significant ($p<0.001$ using one-way ANOVA test). The obtained Hill coefficients indicate WT-like cooperativity of Na^+ binding for p.Leu302Arg (p.L302R), whereas cooperativity was lost for p.Gly303Arg (p.G303R) and p.Met859Arg (p.M859R), as also indicated by the crossing of the line representing the mutant with that of the wild type (WT shown by dotted line in all panels).

FIGURE S2:

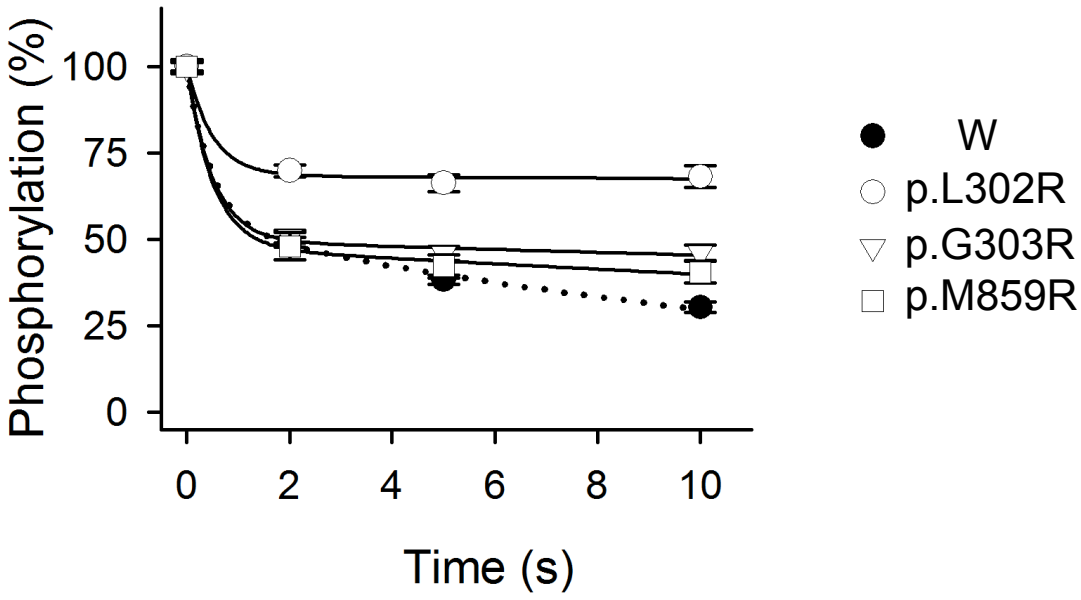

Figure S2: Dephosphorylation of the Na/K-ATPase phosphoenzyme upon addition of ADP for the determination of the distribution of Na^+-bound E1P and the K^+-sensitive E2P form: The amplitude of the rapid phase of dephosphorylation was either WT-like (p.Gly303Arg (p.G303R) and p.Met859Arg (p.M859R)) or reduced in size (p.Leu302Arg (p.L302R)) indicating the presence of more E2P than seen for the WT. These data (n = 13-26) indicate that the reduced K^+ sensitivity observed for all mutants (see figure 2D), is due to a direct effect on K^+ interaction with the E2P state and not caused indirectly by a shift of the E1P-E2P distribution in favor of the K^+-insensitive E1P.

FIGURE S3:

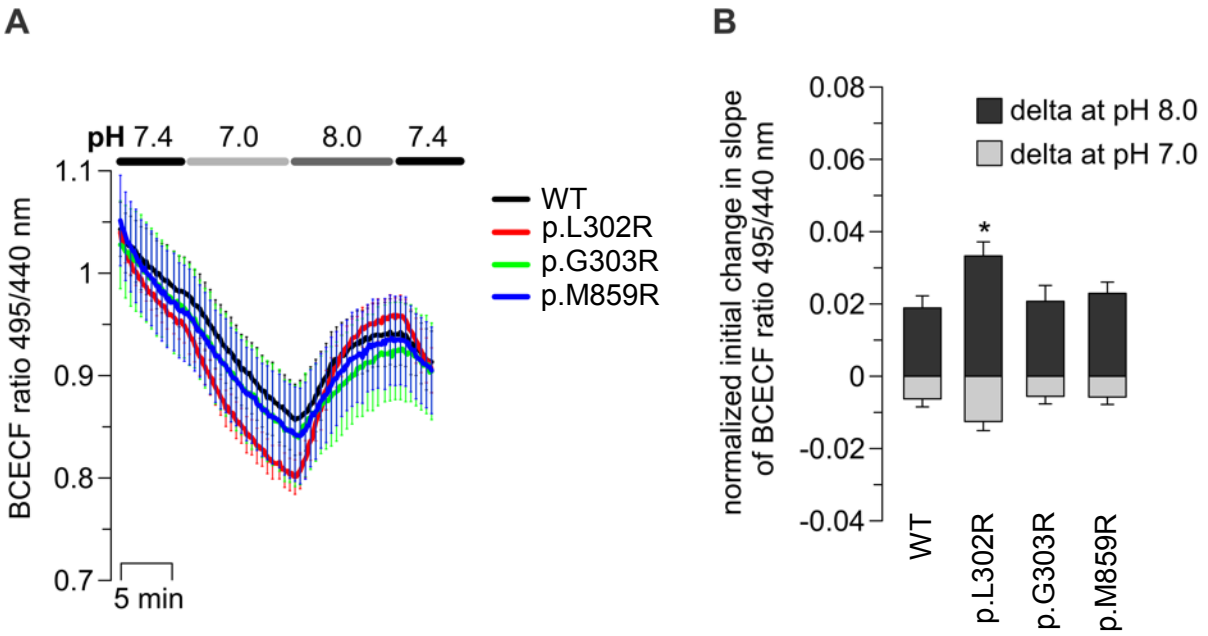

Figure S3: Influence of extracellular pH changes on intracellular pH in adrenal NCI-H295R cells expressing wildtype (WT) or different mutant (p.Leu302Arg (p.L302R), p.Gly303Arg (p.G303R), p.Met859Arg (p.M859R)) ouabain-insensitive rat Atp1a1. Cells were analysed 2 days after transient transfection with *Atp1a1* containing bicistronic plasmids using electroporation. Transfected cells were identified using anti-CD8 coated dynabeads and compared to untransfected cells (devoid of beads) from the same dish. The pH of the extracellular solution was changed from control pH 7.4 to pH 7.0, followed by pH 8.0. The intracellular pH was measured using the pH-sensitive BCECF dye. BCECF ratios (495/440 nm), normalized to the baseline pH of untransfected cells, are show in (A) indicating intracellular acidification by a decreased ratio and alkalinization by an increased ratio, respectively. Expression of the p.Leu302Arg mutant (n=10) led to stronger changes of the intracellular pH upon altering the extracellular pH, whereas p.Gly303Arg (n=7) and p.Met859Arg (n=7) mutant cells were not different from WT cells (n=8). (B) Reactivity of the intracellular pH to alterations of the extracellular pH was quantified by calculating the initial changes in the slope of the BCECF ratio (given here as delta of slope at pH 7.0 and 8.0 compared to the

slope at the end of the pH7.4 control). *$p<0.05$ compared to WT at pH 8.0; n is equal to the number of dishes (measured from different cell passages and at different days of experiments).

SUPPLEMENTAL METHODS AND RESULTS:

PATIENTS

Table S1:

Individual	A-II-1	B-II-1	C-II-2
Origin	of European descent	of European descent	First Nations Canadian
Gender	female	female	male
Age at manifestation	6 months	2 months	6 days
First symptom	generalized seizures	generalized seizures	generalized seizures
<u>Initial laboratory findings:</u>			
S-Na (mmol/L) (136-144)	135	139	141
S-K (mmol/L) (3.6-5.2)	3.8	4.2	2.1
S-Ca (mmol/L) (2.1-2.6)	2.24	2.58	0.9 (ionized, 1.05-1.35)
S-Mg (mmol/L) (0.75-1.1)	0.36	0.35	0.30
S-HCO_3 (mmol/L) (22-26)	26.7	22.0	27.0
Ca/Crea-ratio (mol/mol) (<2.2)	0.24	0.46	4.95
FE-Mg (%) (3-5%)	26.0	33.8	nd
Age at last follow-up	4 years	10 years	6 years
<u>Actual laboratory findings:</u>			
S-Na (mmol/L) (136-144)	136	140	139
S-K (mmol/L) (3.6-5.2)	3.3	3.0	3.9
S-Ca (mmol/L) (2.1-2.6)	2.52	2.23	2.13
S-Mg (mmol/L) (0.75.-1.1)	0.57	0.28	0.62
S-HCO_3 (mmol/L) (22-26)	26.3	25.0	22.0
Ca/Crea-ratio (mol/mol) (<0.9)	0.41	0.40	0.44

FE-Mg (%) (3-5%)	15.3	27.0	21.3
nephrocalcinosis	no	no	no
arterial hypertension	no	no	No
cardiac examination[a]	normal	n.d.	normal
renin (ng/L) (5-67)	53ng/L	n.d.	n.d.
PRA[b] (ng/mL/h) (<7)	n.d.	15.5	1.33
aldosterone (ng/dL) (1-40)	5.2	11.2	1.8
ADRR[c]/ARR[d] (<30)	1.0 (ADRR)	0.7 (ARR)	1.4 (ARR)
seizure activity	repeated status epilepticus	monthly seizures	frequent seizures, repeated status epilepticus
cerebral imaging (MRI)	initially normal, cerebral volume loss during follow-up	normal	mild ventriculomegaly, incomplete myelination
neurological outcome	global developmental delay, hyperactive behavior	global developmental delay, suspected autism spectrum disorder	global developmental delay, speech delay, diagnosis of severe autism, self-biting behaviour
ATP1A1 mutations			
- nucleotide level	c.905T>C	c.907G>C	c.2576T>G
- protein level	p.Leu302Arg	p.Gly303Arg	p.Met859Arg

[a] by electrocardiogram and echocardiography, [b] PRA = plasma renin activity, [c] ADRR = aldosterone-direct renin-ratio, [d] ARR = aldosterone-renin activity-ratio,

Table S1: Clinical Characteristics and Genotypes (complete dataset).

SEQUENCING

The family C trio as well as individual A-II-1 were subjected to whole exome sequencing in separate studies.

Family C was enrolled within the TIDEX gene discovery project (H12-00067), which was approved by the Research Ethics Board of BC Children's and Women's Hospital, University of British Columbia, Vancouver, Canada. Whole exome sequencing was performed for the affected child (C-II-2), mother (C-I-2), and father (C-I-1) of family C. C-II-2 was sequenced using the Agilent SureSelectXT kit and Illumina HiSeq 4000 (Macrogen, South Korea). Mother and father were sequenced using the Agilent V4 51Mb kit and Illumina HiSeq 2000 (Perkin-Elmer, CA, USA). The sequence data was processed and analyzed using a semi-automated pipeline as previously reported [2]. Sequencing reads were aligned to the hg19 human reference genome. Rare variants were assessed for predicted functional impact, using CADD, SIFT and PolyPhen, and were screened under multiple inheritance models. For patient C-II-2, homozygous variants in 9 genes, compound-heterozygous variants in 6 genes, hemizygous variants in 3 genes, and *de-novo* variant in 1 gene were identified.

Singleton exome sequencing of individual A-II-1 was performed from 200ng of genomic DNA. Target enrichment was carried out using the standard protocol SureSelectXT Automated Target Enrichment for Illumina paired-end multiplexed sequencing, and the Agilent Bravo automated liquid handling platform [3]. After validation (2200 TapeStation; Agilent Technologies, CA, USA) and quantification (Qubit System; Invitrogen, Waltham, MA, USA), 2 x 75 bp paired-end reads were sequenced on a HiSeq 4000 (Illumina, San Diego, California). For data analysis, the VARBANK pipeline v.2.15 (unpublished) and the corresponding filter interface was used. Sequence reads were mapped to the hg19/GRCh37 human reference

genome using the Burrows Wheeler Aligner (BWA) alignment algorithm with a mean target coverage of 80 reads per base and 82.4% of targeted bases covered more than 30x.

In individual A-II-1, 4 genes with homozygous variants and 4 genes with more than one potentially pathogenic variant were identified. In addition, the data analysis of individual A-II-1 revealed heterozygous variants in 310 genes.

Comparison of exome data from the two affected individuals (A-II-1 and C-II-2) demonstrated no additional shared gene, beyond *ATP1A1*, with homozygous, compound-heterozygous, or de-novo mode of inheritance. Finally, we also could not identify a gene with a rare heterozygous variant shared by both individuals (A-II-1 and C-II-2).

In contrast, both individuals were found to carry a single heterozygous mutation, p.Leu302Arg and p.Met859Arg in *ATP1A1*, respectively. Targeted Sanger sequencing of index, mother, father and unaffected sibs for family A and C confirmed that both variants occurred *de-novo*. Subsequently, conventional Sanger sequencing of the entire coding region and adjacent exon/intron boundaries of *ATP1A1* revealed a third heterozygous mutation, p.Gly303Arg, in individual B-II-1 that also occurred *de-novo* (see Table S1).

Table S2:

Gene	Individual	Nucleotide change (hg19, cDNA)	Protein change (AA)	Inheritance	SIFT (score)	Polyphen2 (score)
ATP1A1	A-II-1	chr1:116932211 T>G c.905T>G	p.Leu302Arg	heterozygous, *de-novo*	damaging 0.000	probably damaging 0.985
ATP1A1	B-II-1	chr1:116932213 G>C c.907G>C	p.Gly303Arg	heterozygous, *de-novo*	damaging 0.000	probably damaging 1.000
ATP1A1	C-II-2	chr1:116943486 T>G c.2576T>G	p.Met859Arg	heterozygous, *de-novo*	damaging 0.013	possibly damaging 0.561

(RefSeq NM_000701, NP_000692, Transcript ID ENST00000295598, UniProt P05023)

Table S2: Mutations in *ATP1A1*. In silico analyses predicted the variants to be pathogenic (p.Leu302Arg: CADD[4] (32.0); SIFT[5] (Damaging; 0.000); Polyphen2[6] (Probably damaging; 0.985); p.Gly303Arg: CADD (31.0); SIFT (Damaging; 0.000); Polyphen2 (Probably damaging; 1.000); p.Met859Arg: CADD (24.6); SIFT (Damaging; 0.013); PolyPhen2 (Possibly damaging; 0.561)), affecting highly conserved amino acid residues of the Na/K-ATPase α1 protein. None of the identified mutations are listed in publically available exome or genome databases, i.e. ExAC browser (exac.broadinstitute.org) or Genome Aggregation Database (gnomAD) (http://gnomad.broadinstitute.org/).

MEASUREMENT OF Na/K-ATPase ACTIVITY

For biochemical studies, mutations were introduced into full-length cDNA encoding the ouabain insensitive rat α1-isoform of Na/K-ATPase. COS-1 cells were used to express the mutants and wild type, either by the ouabain selection method [7], attempting to obtain stable viable cell lines, or by transient expression in the presence of siRNA to knock down endogenous Na/K-ATPase [8]. Leaky plasma membranes were assayed functionally by previously described methods [1]. Phosphorylation was carried out for 10 s at 0°C with 2 μM [γ-^{32}P]ATP in the presence of varying concentrations of NaCl (100 mM for maximum phosphorylation), 3 mM MgCl, 20 mM Tris (pH 7.5), 100 μM ouabain, and 20 μg oligomycin/ml, or in the presence of 50 mM NaCl, 3 mM MgCl, 20 mM Tris (pH 7.5), 100 μM ouabain, and varying concentrations of KCl with choline chloride added to maintain a constant ionic strength.

For determination of the E1P-E2P-distribution the phosphorylation was carried out in the absence of KCl and dephosphorylation was followed by quenching at various time intervals after addition of 2.5 mM ADP with 1 mM unlabeled ATP. In all phosphorylation experiments the radioactively labeled Na/K-ATPase was separated by acid SDS gel electrophoresis following acid quenching of the reaction mix, and the radioactivity quantified by phosphor imaging.

FUNCTIONAL STUDIES

Plasmids containing full-length cDNA sequences encoding wild-type or mutant ouabain-insensitive rat *Atp1a1* were generated as described [8, 9]. Adrenocortical carcinoma NCI-H295R cells (CLS) were transfected using electroporation as described [9]. Cells were analyzed 48

hours after transfection. For patch-clamp, pH, and Ca^{2+} measurements, transfected cells were identified using anti-CD8-coated dynabeads (Life Technologies GmbH).

Whole-cell patch recordings were performed at room temperature using an EPC 10 amplifier (Heka), relative cytosolic pH levels were measured using the ratiometric fluorescent pH sensitive dye BCECF-AM (Life Technologies GmbH) as described [9]. For Na^+-free extracellular conditions, bath Na^+ was replaced by N-methyl-D-glucamine ($NMDG^+$). In addition, flame photometry was used for the determination of intracellular Na^+ and K^+ contents as described [10]. Intracellular Na^+ and K^+ contents were measured under control conditions and after treatment with 10 µM ouabain inhibiting endogenous human ATP1A1 but not the transfected ouabain-insensitive rat ATP1A1. Cultured cells were washed with a Na^+-free solution before swelling and disruption of cells was induced by incubation in MilliQ-water on ice for 1.5 hours. Cell lysates are homogenized mechanically and cleared from cellular debris by centrifugation. Finally, Na^+- and K^+ concentrations in the supernatant were measured using flame photometry (PFP7 Industrial Flame Photometer, Jenway/Cole Parmer, Staffordshire, UK). Ion concentrations were calculated as ratios of Na^+- or K^+ content, respectively, compared to the sum of Na^+ and K^+ content.

STATISTICAL ANALYSIS

Phosphorylation data were analyzed using the SigmaPlot program (SPSS, Inc.) for non-linear regression using the Hill equation for cooperative binding [1]. Statistical significance was tested using Student's t test (for paired or unpaired samples as appropriate). All data are presented as mean ± SEM. For multiple comparisons, an ANOVA plus Bonferroni or Holm-Sidak post-hoc test was used. Differences between groups were considered significant if $p<0.05$ for single comparisons or $p<0.01$ for multiple comparisons.

LITERATURE

1. Toustrup-Jensen, M.; Hauge, M.; Vilsen, B., Mutational effects on conformational changes of the dephospho- and phospho-forms of the Na+,K+-ATPase. *Biochemistry* **2001,** *40* (18), 5521-32.

2. Tarailo-Graovac, M.; Shyr, C.; Ross, C. J.; Horvath, G. A.; Salvarinova, R.; Ye, X. C.; Zhang, L. H.; Bhavsar, A. P.; Lee, J. J.; Drogemoller, B. I.; et al., Exome Sequencing and the Management of Neurometabolic Disorders. *N Engl J Med* **2016,** *374* (23), 2246-55.

3. Altmuller, J.; Motameny, S.; Becker, C.; Thiele, H.; Chatterjee, S.; Wollnik, B.; Nurnberg, P., A systematic comparison of two new releases of exome sequencing products: the aim of use determines the choice of product. *Biol Chem* **2016,** *397* (8), 791-801.

4. Kircher, M.; Witten, D. M.; Jain, P.; O'Roak, B. J.; Cooper, G. M.; Shendure, J., A general framework for estimating the relative pathogenicity of human genetic variants. *Nat Genet* **2014,** *46* (3), 310-5.

5. Ng, P. C.; Henikoff, S., Predicting deleterious amino acid substitutions. *Genome Res* **2001,** *11* (5), 863-74.

6. Adzhubei, I. A.; Schmidt, S.; Peshkin, L.; Ramensky, V. E.; Gerasimova, A.; Bork, P.; Kondrashov, A. S.; Sunyaev, S. R., A method and server for predicting damaging missense mutations. In *Nat Methods*, United States, 2010; Vol. 7, pp 248-9.

7. Vilsen, B., Glutamate 329 located in the fourth transmembrane segment of the alpha-subunit of the rat kidney Na+,K+-ATPase is not an essential residue for active transport of sodium and potassium ions. *Biochemistry* **1993,** *32* (48), 13340-9.

8. Beuschlein, F.; Boulkroun, S.; Osswald, A.; Wieland, T.; Nielsen, H. N.; Lichtenauer, U. D.; Penton, D.; Schack, V. R.; Amar, L.; Fischer, E.; et al., Somatic mutations in ATP1A1 and ATP2B3 lead to aldosterone-producing adenomas and secondary hypertension. *Nat Genet* **2013,** *45* (4), 440-4, 444e1-2.

9. Stindl, J.; Tauber, P.; Sterner, C.; Tegtmeier, I.; Warth, R.; Bandulik, S., Pathogenesis of Adrenal Aldosterone-Producing Adenomas Carrying Mutations of the Na(+)/K(+)-ATPase. *Endocrinology* **2015,** *156* (12), 4582-91.

10. Tauber, P.; Aichinger, B.; Christ, C.; Stindl, J.; Rhayem, Y.; Beuschlein, F.; Warth, R.; Bandulik, S., Cellular Pathophysiology of an Adrenal Adenoma-Associated Mutant of the Plasma Membrane Ca(2+)-ATPase ATP2B3. *Endocrinology* **2016,** *157* (6), 2489-99.